Lawrence Berkeley National Laboratory
Recent Work

Title
THE SURFACE CHEMISTRY OF THE THERMAL CRACKING OF SILANE ON (111) SILICON

Permalink
https://escholarship.org/uc/item/3dz6b431

Authors
Farnaam, M.K.
Olander, D.R.

Publication Date
1983-10-01

eScholarship.org Powered by the California Digital Library
University of California

UC-4
LBL-16921
Preprint c.1

Lawrence Berkeley Laboratory

UNIVERSITY OF CALIFORNIA

Materials & Molecular Research Division

RECEIVED
LAWRENCE
BERKELEY LABORATORY
FEB 1 1984
LIBRARY AND
DOCUMENTS SECTION

Submitted to Surface Science

THE SURFACE CHEMISTRY OF THE THERMAL CRACKING OF SILANE ON (111) SILICON

M.K. Farnaam and D.R. Olander

October 1983

For Reference

Not to be taken from this room

Prepared for the U.S. Department of Energy under Contract DE-AC03-76SF00098

LBL-16921 c.1

DISCLAIMER

This document was prepared as an account of work sponsored by the United States Government. While this document is believed to contain correct information, neither the United States Government nor any agency thereof, nor the Regents of the University of California, nor any of their employees, makes any warranty, express or implied, or assumes any legal responsibility for the accuracy, completeness, or usefulness of any information, apparatus, product, or process disclosed, or represents that its use would not infringe privately owned rights. Reference herein to any specific commercial product, process, or service by its trade name, trademark, manufacturer, or otherwise, does not necessarily constitute or imply its endorsement, recommendation, or favoring by the United States Government or any agency thereof, or the Regents of the University of California. The views and opinions of authors expressed herein do not necessarily state or reflect those of the United States Government or any agency thereof or the Regents of the University of California.

LBL-16921

October, 1983

THE SURFACE CHEMISTRY OF THE THERMAL CRACKING OF SILANE ON (111) SILICON

M.K.FARNAAM

AND

D.R. OLANDER

Molecular and Materials Research Division, Lawrence Berkeley Laboratory
and Department of Nuclear Engineering, College of Engineering;
University of California, Berkeley, California 94720

This work was supported by the Director, Office of Energy Research,
Office of Basic Energy Sciences, Materials Sciences Division of the
U.S. Department of Energy under Contract No. DE-AC03-76SF0098.

ABSTRACT

The kinetics of the thermal decomposition of silane gas during epitaxial growth on the (111) face of single crystal silicon were studied by modulated molecular beam mass spectrometry over the temperature range of 1000 K - 1440 K and with beam intensities from 2 x 20^{15} to 2 x 10^{16} molecules/cm^2-s. An abrupt change in the apparent reaction probability was observed at ~ 1130 K, coinciding with a known surface structural transformation at about the same temperature. The molecular beam data for temperatures higher than 1130 K were used for construction of a reaction model. Additional experiments were conducted to fix certain features of the reaction mechanism. An attempt was made to measure the rate constant for desorption of unreacted silane molecules from the surface. The residence time of silane on the surface was below the sensitivity limit of the technique (< 5 μs), which means that SiH_4 desorption is not rate-limiting. Application of a simultaneous modulated beam of SiH_4 and a steady beam of SiD_4 did not produce HD molecules, thus ruling out hydrogen atom production in the surface reaction mechanism. According to the proposed model, silane molecules which do not reflect from the surface undergo a branched reaction with two types of sites on the surface, producing two bound SiH_2 molecules in each chemisorption event. Subsequent surface decomposition of the adsorbed SiH_2 molecules occur with different pre-exponential factors, although with similar activation energies of about 17 kcal/mole for the two types of sites.

I. INTRODUCTION

Epitaxial growth of silicon via thermal cracking of silane by the overall reaction $SiH_4(g) \rightarrow Si + 2H_2(g)$ can be divided into two subprocesses: (1) the surface decomposition of the silicon-bearing gas to produce adsorbed silicon atoms, and (2) the incorporation of silicon adatoms into an epitaxial layer. The second aspect has received the most attention in the literature (1-3); the growth process is driven by the supersaturation of the surface with silicon adatoms but does not depend upon their source (i.e. whether produced from a CVD process or by condensation of silicon vapor). The first subprocess contains all the surface chemistry of the overall process, and is the subject of the present study.

Henderson and Helm (4) investigated silane decomposition on silicon in a conventional kinetic experiment at silane pressures from 0.02 to 0.15 Torr and at temperatures from 1070 to 1220 K. The change of pressure with time determined the rate of silane cracking. The silane decomposition rate and the film growth rate depended linearly on pressure and exhibited an activation energy of 20 ± 5 kcal/mole. Their model of the chemistry involved simple cracking of SiH_4 to produce gaseous H_2 and silicon adatoms. The latter either desorbed to the gas phase or joined the surface crystal structure.

In a series of experiments, Joyce and coworkers used the molecular beam technique to investigate silane reaction kinetics on Si (111) (5-7). Mass spectrometry was used to follow the H_2 partial pressure as a function of silane beam intensity and substrate temperature. An activation energy of 18.7 ± 2 kcal/mole and a reaction order near two were determined. Their reaction model involved an initial SiH_4 decomposition

step which produced SiH_3 and H adsorbed surface species. Subsequent surface reactions of these species led to gaseous H_2 and silicon atoms.

Farrow's study (8) employed a gas-flow technique with molecular beam sampling. The silane decomposition rate depended linearly on silane pressure and exhibited an activation energy of 17 ± 2 kcal/mole. The results were interpreted with a mechanism similar to that proposed by Henderson and Helm (4).

Joyce et al. (5 - 7) described the advantages of applying the molecular beam technique to investigate this reaction. This method was chosen for the present study with the additional feature of beam modulation to provide direct measurement of the kinetics of the surface steps. Substrate growth rates were not measured; the primary goal of the present study was to elucidate the kinetics and mechanism of the chemical reactions which produced silicon adatoms from SiH_4. This was accomplished by monitoring the H_2 product of the decomposition.

In the modulated molecular beam-mass spectrometric method, phase-sensitive detection electronics process the signals according to the shapes and magnitudes of the waveforms and produce the phase angles and amplitudes of the first Fourier components. The phase information is related to the time lag between reactant incidence on and product emission from the surface and thus contains valuable kinetic information. This feature constitutes the main advantage of the modulated beam technique over the conventional steady state kinetic methods. The relative amplitude of the product and reactant signals is a measure of the fraction of the incident molecules which react to form a particular product molecule. The apparent reaction probability (ε) is the ratio of the

amplitudes of the first Fourier components of the product and scattered reactant signals. The phase lag (ϕ) is the difference in the phase angles of the same Fourier components. These two quantities are determined experimentally as functions of the frequency of modulation (f), the intensity of the reactant beam (I_0), and the temperature of the solid (T).

Theoretically, surface reaction models are analyzed to provide predictions of ε and ϕ as functions of the same three experimental variables. The parameters which characterize the elementary steps of a reaction model include the reactant gas sticking probability, reactive site densities on the surface, and the preexponential factors and activation energies of all temperature-dependent quantities such as rate constants and diffusion coefficients. Values of the model's parameters are determined by fitting the theoretical calculation to the experimental results. It is customary to examine several theoretical models and choose the one which best fits the data and requires the least number of parameters.

The experimental responses often serve as guides to model development. For example, the phase lag usually approaches zero as $f \to 0$ and tends to a limiting value at high modulation frequencies. For simple product desorption-controlled kinetics, the limiting phase lag is 90°, while for a series process on the surface, the limit is 180°. If increasing the beam modulation frequency results in a decrease or a maximum in the phase lag, the surface reaction involves a branched process. For a reaction totally controlled by a diffusional step, the phase lag is 45°, independent of all experimental parameters. These "signatures" of particular elementary steps in complex reaction sequences have been cataloged by a number of authors, along with dicussions of

the advantages of the modulated beam method, its limitations, potential improvements and equipment alternatives (9 - 13). The technique has been applied in quite a few experimental studies of gas-solid reactions, some of which can be found in Refs. 14 - 20.

Residence time of silane molecules on the silicon surface has been a source of controversy among the kinetic studies described above. Joyce et al.(5 - 7) and Henderson and Helm (4) believe that cracking of silane occurs during collision with the crystal surface, whereas in Farrow's model (8) cracking follows adsorption of silane on the surface. Whenever a silane molecule strikes the silicon surface, it either scatters back to the gas, cracks to release hydrogen, or absorbs with subsequent cracking or desorption. Although desorbed silane cannot be distinguished from scattered silane in a steady state experiment, these two classes of SiH_4 can be differentiated by virtue of modulation of the incident beam. The part of the silane flux which scatters from the surface does so instantaneously, or with no phase lag ascribable to residence on the surface. On the other hand, silane which physically adsorbs on the surface and then desorbs can be characterized by a mean surface lifetime τ, which produces a phase lag $2\pi f\tau$ in this component of the silane flux leaving the silicon surface. The amplitude and phase lag of the silane signal observed by the phase-sensitive detector is the vector sum of the scattered and desorbed portions. Using a mixed beam of silane and an inert gas and measuring the phase difference between the two as a function of modulation frequency provides a means analyzing SiH_4 adsorption-desorption in the presence of scattering.

Another aspect of the mechanism of SiH_4 cracking left unresolved by the previous studies is the question of whether hydrogen atoms are produced on the surface during reaction. Were this to take place, part of the

measured H_2 emission would arise from surface recombination of hydrogen adatoms. This form of H_2 can be distinguished from H_2 produced directly by silane cracking on the surface by an isotope mixing experiment. A steady beam of SiD_4 is directed on the surface simultaneously with a modulated beam of SiH_4 of comparable intensity. If hydrogen atoms are produced on the surface then there should be a production rate of HD comparable to that of H_2 or D_2 due to the recombination process. On the other hand, if the decomposition process involved simply splitting SiH_4 molecules into Si and two H_2 molecules, no HD should be produced in the isotope mixing experiment.

II EXPERIMENTAL

The modulated molecular beam apparatus is shown in Fig. 1. The beam source is a quartz tube terminating in a 1 mm thick membrane with a 0.5 mm diameter hole. The tube contains semiconductor-grade silane gas at pressures between 0.1 and 1 Torr. The gas flux from the source is collimated by a 0.8 mm diameter orifice into a thin beam which impinges on a solid target. The chamber containing the target is pumped to high vacuum ($\sim 10^{-8}$ Torr), so impingement of background gases is much smaller than the rate at which beam molecules strike the surface. The latter is equivalent to pressures up to 10^{-4} Torr. The pressure of silane in the source tube controls the flow rate from the hole and hence the intensity of the molecular beam which strikes the target. The relationship between the silane pressure in the source and the beam intensity was determined in separate tests in which the target was removed to allow the molecular beam to enter a closed ion gauge tube at the rear of the chamber. The beam intensity at the position of the target was calculated from the pressure rise measured by the ion gauge tube for various gas pressures in the source tube. The range of SiH_4 beam-intensities begins with a value large enough to distinguish the reaction product

signal from noise. The maximum beam intensity is limited by the pumping power of the vacuum system and by corrosive attack by silane on sensitive components in the system. However, the order-of-magnitude accessible range of beam intensity is sufficient to reveal any nonlinearity in the reaction kinetics.

Before formation into a molecular beam, the reactant gas effusing from the source tube passes through the rotating blades of a toothed disk. The range of modulation frequencies is dictated by the mechanical stability of the chopper at low frequencies is by the limitations of chopper driver power at high frequencies. In addition, transit time effects provide a natural upper limit; when the transit times of molecules between source and target and between target and detector become long compared to the characteristic reaction times of the surface processes, the measured phase lags are dominated by the former, thereby masking the small effects due to surface reactions. Fortunately, the accessible modulation frequency range (20-900 Hz) was well-matched to the characteristic response times of the surface reactions responsible for silane cracking.

The target is a chip of a single-crystal silicon produced by Epitaxy Inc. This material was prepared by the supplier by deposition of a 0.6 μm thick undoped silicon epitaxial layer on a 375 μm thick single crystal silicon wafer with (111) faces. A triangular sample with 17 mm sides parallel to the [110] directions was broken from the wafer using a sharp object. Aside from a slight blow of nitrogen gas to clean the surface, the crystal was used in the as-received condition. The target was placed on top of a tantalum ring with the epitaxial layer facing the incident beam

and heated by electron bombardment. The temperature was measured by an optical pyrometer sighted on the target surface. Emissivities at the pyrometer wavelength were taken from Ref. 21. The maximum temperature (1443 K) is an upper limit for well-controlled heating of the specimen without risking melting. Below $\sim$1000 K, no reaction was detectable.

To verify that the sample was free of contamination (principally carbon), it was annealed at temperatures between 1400 and 1600 K for an hour at ambient vacuum pressures of $\sim 10^{-8}$ Torr. Following this treatment, the sample appeared as bright as before and examination by scanning electron microscopy revealed a featureless surface. The triangular pits or surface lumps which result from vaporization of a contaminated surface (22, 23) were absent. Similar tests were performed under deposition conditions, 1400 K with a SiH_4 beam of 1 - 3 x 10^{15} molecules/cm^2-s, with the same results. The absence of surface morphology following these tests indicated that silicon atoms were added or removed from the (111) surface by a layer-by-layer process. These samples were therefore judged to be sufficiently clean for chemical kinetic studies. Following the molecular beam experiments, the target surfaces were again examined by SEM; none showed any surface morphology, which is an indication of the adequacy of experimental conditions such as beam purity, background gas pressure, and contamination of the surface by bulk diffusion of impurities from the silicon or by surface diffusion from the structures supporting the target. In all cases, only two-dimensional, featureless growth of the silicon crystal substrate occurred in the central portion of the specimen. Near the edges where clips held the crystal, the surface was pitted due to impurities arising from the support structure. It should be noted that the requirement of featureless surfaces following high temperature growth or evaporation is a much more stringent test of surface cleanliness than achievable with Auger electron spectroscopy which has a detection limit of a few percent of a monolayer. Surfaces which

appear carbon-free by AES can become pitted at high temperatures due to undetectable impurities.

For the isotope mixing tests, provision was made for simultaneously injecting SiD_4 directly onto the target surface. This was accomplished by a copper doser tube located 1 cm away from the surface. The SiD_4 impingement rate on the target was calculated from the supply pressure and the flow resistance of the tubing.

Chopping of the incident beam induces modulation at the same frequency in the product species desorbed from the target. Following recollimation, both the reflected reactant and desorbed products are detected by a quadrupole mass spectrometer located in the third chamber of Fig. 1. The 1.6 mm diameter orifice separating the target chamber from the detection chamber insures that the sampling beam does not collide with the walls of the ionizer of the mass spectrometer. Neutrals and mass-analyzed ions travel along the mass filter but at the exit the selected ions are deflected towards the input face of the electron multiplier. The neutral species continue undeviated and are either deposited on the chamber walls or removed by the pumps. This separation significantly reduces the electronic noise which is produced when the neutral species is allowed to enter the electron multiplier input.

The output of the electron multiplier and the reference signal from the optical switch monitoring chopper rotation are fed to a lock-in amplifier augmented with a two-phase accessory. This combination Fourier-analyzes the signal from the electron multiplier and produces the phases and amplitudes of the various modes into which the complete signal waveform is decomposed. Only the fundamental mode was used in this study.

The output signals from the mass spectrometer had to be analyzed to determine the relative proportions of the reaction product H_2 and the scattered reactant SiH_4. This procedure was not straightfoward because

fragmentation of SiH_4 molecules by the 33 volt electrons used in the mass spectrometer ionizer produced SiH_4^+, SiH_3^+, SiH_2^+, SiH^+, Si^+ and H_2^+. Of these, the SiH_2^+ signal is the largest, but the presence of H_2^+ from SiH_4 cracking complicates quantitative detection of H_2. The ionization potential of H_2 is higher than the appearance potential of H_2^+ from SiH_4, so it is not possible to select an appropriately low ionizing electron energy to avoid cracking of SiH_4 without rendering the H_2 product undetectable.

Silicon has three stable isotopes, Si^{28} (92.2%), Si^{29} (4.7%), and Si^{30} (3.1%). Therefore the signal measured by tuning the mass spectrometer to mass 30 consists not only of $Si^{28}H_2^+$ ions, but also includes $Si^{29}H^+$ and Si^{30+}. However, knowing that the mass-30 signal represents 42% of the sum of the signals from all fragments of SiH_4 ionization, the former can be used as a direct measure of the silane content of the gas emanating from the target surface. The mass-2 signal consists solely of H_2^+, but as noted above, only partly arising from reaction product H_2. Below about 1000 K the mass-2/mass-30 signal ratio was constant at a value of a few percent. At higher temperatures, this ratio increased significantly, indicating the onset of silane cracking on the silicon target. The mass-2 signal also exhibited a phase lag with respect to the mass-30 signal above 1000 K, but none at lower temperatures. The task of determining the portions of the mass-2 signal (amplitude and phase) which were due to cracking of silane by the surface and in the mass spectrometer was accomplished by a computer program which used the signals measured with the target at room temperature as well as at the high temperature of the experiment. This procedure directly yielded the phase lag of the H_2 reaction product relative to the incident SiH_4 reactant.

The final piece of data needed for determination of the apparent reaction probability was the ratio of the ionization cross sections of H_2 to SiH_4. The former is known (24) and the latter was measured in the apparatus of Fig. 1 by removing the target and installing a nozzle aimed directly into the mass spectro-

meter ionizer. By comparing the mass spectrometer responses to known flow rates of N_2 and SiH_4 from this nozzle, the SiH_4 ionization cross section relative to that of N_2 was obtained. From this information the ionization cross section ratio of H_2 to SiH_4 was determined. This quantity affects only the apparent reaction probability but not the phase lag deduced from the mass spectrometer signals.

Additional details of the apparatus and data interpretation methods are available in Refs. 17 and 25.

III RESULTS

The controllable variables in a modulated molecular beam experiment are the specimen temperature, modulation frequency and incident reactant beam intensity. An experimental campaign consists of fixing two of these variables and varying the third over its accessible range. For each experiment, the apparent reaction probability and phase lag of the reaction product H_2 relative to the SiH_4 reactant were determined. Some of the tests were repeated several times, which permitted estimates of the precision to be made. Based on these replications, error bars have been assigned to the data points. The molecular beam data are shown in Figs. 2-5 along with theoretical curves which will be discussed in the next section. Two frequency scans were performed, one at 1243 K (Fig. 2) and the other at 1443 K (Fig. 3). The behavior of the phase lag with respect to modulation frequency at both temperatures strongly indicates the existence of a branch process in the mechanism.

Figure 4 shows the lack of influence of the incident silane beam intensity on the reaction product vector. At 1443 K and 20 Hz, this observation suggests that the elementary steps of the model consist only of first order reactions, and eliminates coverage-dependence of the sticking probability of SiH_4 on Si. Gelain et al. (26) also reported a pressure-

independent reaction probability for the decomposition of silane on silicon at 1183 K for silane pressures up to 10^{-4} Torr.

The temperature dependence of the reaction product vector is shown in Fig. 5. As can be seen from this plot, the apparent reaction probability is almost independent of temperature above about 1130 K and then decreases sharply at lower temperatures. An analogous change is also apparent in the phase lag. Madix and Schwarz (18) reported similar abrupt changes in the reaction probability and phase lag at around 1050 K for the reaction of molecular chlorine with the (111) face of single crystal silicon. The chemical reactivity transition temperature of 1130 K in Fig. 5 falls within the temperature region from 1130 to 1180 K where the (111) surface undergoes a transformation from an ordered 7x7 structure to a featureless 1x1 structure (27, 28).

Beyond the surface transition temperature the apparent reaction probability is nearly constant and the phase lag is low. This behavior is characteristic of a reaction which is nearly supply-limited, by which is meant that all surface steps following initial sticking of the gaseous reactant are rapid and the emission of reaction product is directly dependent on the rate of reactant supply to the surface. In this limit, the apparent reaction probability is twice the sticking probability (because each interaction of an SiH_4 molecule with the surface produces two molecules of H_2) and, as seen from Fig. 4, independent of incident beam intensity. Fortunately, the surface reactions are not so fast that the phase lag vanishes. Figure 5 shows that ϕ is between 10 and 20 degrees at 20 Hz and Figs. 2 and 3 show that the phase lag rises to $\sim 60^{o}$ at high modulation frequencies. The constancy of the phase lag in Fig. 4 is the true indicator of a mechanism with only linear steps. Therefore, kinetic information is

still extractable from the phase lag data even though the high temperature reaction probability data serve only to give the total sticking probability of SiH_4 on Si(111).

The attempt to characterize adsorption-desorption of unreacted silane on the Si(111) surface was based on measuring the phase difference between the two species in an argon/silane mixed beam. Sufficiently long holdup of silane due to adsorption followed by slow desorption should cause the silane signal to lag behind that of the reflected argon. Figure 6 shows the results of such a test at two substrate temperatures. Contrary to expectations, the SiH_4 signal leads rather than lags the inert gas signal. Similar behavior occurs when the temperature of the target was near ambient, and in fact, with silane replaced by neon. The negative phase lags are attributed to experimental uncertainties and the results mean that the adsorption-desorption properties of silane on silicon were not observable. This finding has two interpretations. Either SiH_4 does not physically adsorb on Si(111) (it either scatters or cracks) or the physically adsorbed silane has such a short residence time (less than a few microseconds) that it is not detectable at the modulation frequencies where transit phase lags do not dominate the entire process (e.g. $f < 900$ Hz).

The experiments utilizing simultaneous impingement of modulated SiH_4 and steady SiD_4 beams were conducted over a wide range of intensities from each source and over the temperature interval 1143 to 1443 K. In no case was modulated HD detected in the hydrogen reaction products. From this negative result it can be concluded that atomic hydrogen is not a surface intermediate in silane cracking, for if it were, it would have produced HD under the conditions of the isotope mixing tests.

IV DISCUSSION

Construction of a model of the surface reaction is based on the features of the experimental results discussed in the preceding section. Specifically, the mechanism appears to contain parallel pathways for production of the same product (H_2), all steps are linear, slow desorption of physically adsorbed silane is not important, and hydrogen atoms are not surface species of any significance. Because of the paucity and poor quality of the data taken at temperatures below the surface transition, the model applies only for T > 1130 K.

The following model conforms to these restrictions:

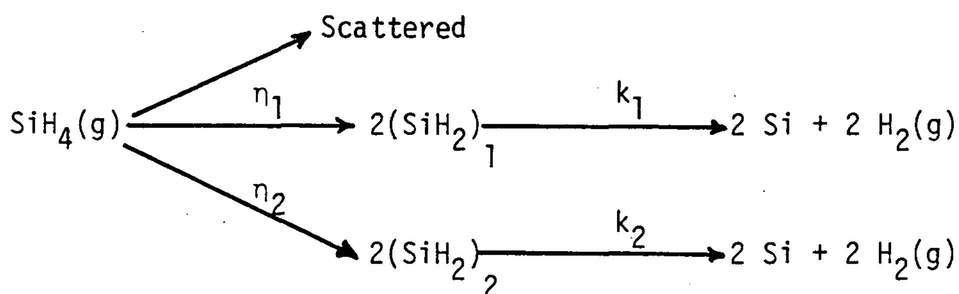

a silane molecule striking the surface is either reflected or combines with a surface silicon atom to form two adsorbed SiH_2 molecules. The latter process can take place on either one of two types of surface sites, denoted as 1 and 2. Figure 5 suggests that the sticking probabilities η_1 and η_2 are independent of temperature, which implies that neither the surface densities of the sites nor the cracking of SiH_4 into SiH_2 are thermally activated. Sites 1 and 2 must be sufficiently different in atomic structure that subsequent decomposition of SiH_2 takes place with different rate constants, denoted by k_1 and k_2, respectively. This kinetic distinction might arise from differences in the geometrical arrangements of lattice atoms which are nearest neighbors of the SiH_2 molecule in the two

types of sites. This could affect properties such as the Si-H vibrational frequency (29), which in turn could influence the SiH_2 decomposition rate constant. The two types of sites in the reaction model might be identified with kinks and ledges, respectively, on the unreconstructed (111) face of the silicon crystal during the two-dimensional layer-by-layer epitaxial growth process. Kinks and ledges have one of the attributes of the two reactive sites postulated in the model, namely, that of temperature-independent surface densities.

Neglecting coverage-dependence of the sticking probabilities, the surface mass balance equations for the model can be written as:

$$\frac{dn}{dt} = 2\eta_1 I_o g(t) - k_1 n$$

$$\frac{dm}{dt} = 2\eta_2 I_o g(t) - k_2 m \qquad (1)$$

where n and m are the surface number densities of the SiH_2 intermediates on sites 1 and 2, respectively, and I_o is the amplitude of the incident SiH_4 beam. The gating function of the modulated beam is represented by g(t), which is approximately a square wave of period 1/f.
The time dependences of n,m, and g are periodic, and Fourier expansion up to the first mode yields:

$$n(t) = n_o + \bar{n}_1 e^{i2\pi ft}$$

$$m(t) = m_o + \bar{m}_1 e^{i2\pi ft} \qquad (2)$$

$$g(t) = \frac{1}{2}(1 + g_1 e^{i2\pi ft})$$

where $g_1 = 4/\pi$ for an incident square wave. The steady state densities n_o and m_o are real whereas the quantities $\bar{n}_1$ and $\bar{m}_1$, representing the first Fourier components, are complex. The reaction product vector is

defined as the ratio of the fundamental modes of the rate of production of H_2 to the rate of SiH_4 impingement:

$$\varepsilon\, e^{-i\phi} = \frac{k_1\bar{n}_1 + k_2\bar{m}_1}{\frac{1}{2}\, g_1 I_o} \quad . \tag{3}$$

Equations (2) are substituted into Eqs(1) and the solutions for $\bar{m}_1$ and $\bar{n}_1$ are inserted into Eq(3). This procedure yields the following formulas for ε and ϕ:

$$\begin{aligned} \varepsilon &= 2(x^2 + y^2)^{\frac{1}{2}} \\ \phi &= \tan^{-1}(y/x) \end{aligned} \tag{4}$$

where

$$\begin{aligned} x &= \frac{\eta_1}{1+a_1^2} + \frac{\eta_2}{1+a_2^2} \\ y &= \frac{\eta_1 a_1}{1+a_1^2} + \frac{\eta_2 a_2}{1+a_2^2} \end{aligned} \tag{5}$$

and

$$\begin{aligned} a_1 &= 2\pi f/k_1 \\ a_2 &= 2\pi f/k_2 \end{aligned} \tag{6}$$

In addition to the rate constants, the ε and ϕ formulas contain the modulation frequency. The beam intensity does not appear because the system of equations is linear. The temperature is implicit in the Arrhenius forms of the rate constants.

Date fitting was performed by using a computer program which minimizes the sum of normalized squares of the errors in ϕ and the logarithm of ε. The fitting procedure resulted in the following set of parameters:

$\eta_1 = 0.038$

$\eta_2 = 0.068$

$$k_1 = 5.1\times10^4 \exp(-16.3/RT),\ s^{-1}$$
$$k_2 = 4.6\times10^6 \exp(-17.8/RT),s^{-1}\ .$$

where the activation energies are in kcal/mole and R is the gas constant. The theoretical curves for ε and ϕ based on these model parameter values are shown in Figures 2-5. Agreement with the data is satisfactory except for temperatures below ~1200K, which, however, is close to the temperature range of the surface structural transformation.

Three other sets of reaction parameters were also found which fit the data in a visual sense nearly as well as the set given above. However, these alternate reaction parameters exhibited poorer least squares agreement with the data than the best-fit set. The rate constants for these sets of parameters are shown as lines A, B, and C in Fig. 7 along with the rate constants of the best fit. Although the magnitudes of the rate constants in each group are within a factor four of each other, their preexponential factors and activation energies are drastically different. The insensitivity of the experimental reaction probabilities to temperature (Fig. 5) leaves only the frequency responses of ϕ at two temperatures (Figs. 2 and 3) from which the temperature behavior can be inferred. This results in the substantial variances in preexponential factors and activation energies even though the absolute magnitudes of k_1 and k_2 are in close accord. Despite this shortcoming, the activation energies are in good agreement with those determined in earlier studies, which ranged from 17 to 20 kcal/mole (4-8). The total silane sticking probability of ~0.1 is also consistent with previous work.

V CONCLUSIONS

Modulated molecular beam experiments have been conducted and the results interpreted in terms of a mechanistic model of the reaction of silane with the (111) face of single crystal silicon in the temperature range of 1130K to 1443K. Isotope mixing and silane adsorption-desorption tests, although producing negative results, aided in model development. In the model, silane molecules which do not reflect from the surface undergo a branched reaction with two types of sites on the surface. Each chemisorption event produces two bound SiH_2 molecules which decompose into Si and H_2 with different rate constants.

Molecular beam data obtained at temperatures below 1130K were not sufficiently precise to warrant reaction modeling. However, the dramatic decrease in reactivity compared to the high temperature reaction probably resulted from surface structural transformation which is known to occur at about the same temperature.

Acknowledgement

Both authors would like to thank Dr. B. A. Joyce for his interest in this work and for his helpful suggestions for overcoming the persistent problem of achieving contaminant-free surfaces. This work was supported by the Director, Office of Energy Research, Office of Basic Energy Sciences, Materials Sciences Division of the U.S. Department of Energy under contract #DE-AC03-76SF00098.

REFERENCES

1. H. C. Abbink, R. M. Broudy and G. P. McCarthy, J. Appl. Phys. 39 (1968), 4673.
2. M. Shimbo, J. Nishizawa and T. Terasaki, J. Crystal Growth 23 (1974), 267.
3. E. I. Giravgizov, J. Crystal Growth 52, 194 (1981).
4. R. C. Henderson and R. F. Helm, Surf. Sci. 30 (1972), 310.
5. B. A. Joyce and R. R. Bradley, Phil. Mag. 14 (1966), 289.
6. C. R. Booker and B. A. Joyce, Phil. Mag. 14 (1966), 301.
7. B. A. Joyce and R. R. Bradley, Phil. Mag. 15 (1967), 1167.
8. R. F. C. Farrow, J. Electrochem. Soc. 121 (1974), 899.
9. R. H. Jones, D. R. Olander, W. J. Siekhaus and J. A. Schwartz, J. Vac. Sci. Technol. 9 (1972), 1429.
10. C. T. Foxon, M. R. Boudry, and B. A. Joyce, Surf. Sci. 44 (1974), 69.
11. J. A. Schwartz and R. J. Madix, Surf. Sci. 46 (1974) 317.
12. R. L. Palmer and J. N. Smith, Jr., Catal. Rev. 12 (1975), 279
13. D. R. Olander, J. Colloid and Interface Sci. 58 (1977), 169.
14. C. T. Foxon and B. A. Joyce, Surf. Sci. 50 (1975), 434.
15. S. L. Bernasek and G. A. Somorjai, J. Chem. Phys. 62 (1975), 3149.
16. R. J. Madix, in "Physical Chemistry of Fast Reactions" Vol. 2, D. O. Hayward, Ed., Plenum Press, (1975).
17. A. J. Machiels and D. R. Olander, Surf. Sci. 65 (1977), 325.
18. R. J. Madix and J. A. Schwartz, Surf. Sci. 24 (1971), 264-287.
19. M. Balooch and D. R. Olander, J. Electrochem. Soc. 130 (1983), 151.
20. G. E. Gdowski, J. A. Fair and R. J. Madix, Surf. Sci. 127 (1983), 541.
21. F. G. Allen, J. Appl. Phys. 28 (1957), 1510.
22. Private communication from B. A. Joyce, 1978.
23. R. C. Henderson, R. B. Marcus, and W. J. Polito, J. Appl. Phys. 42 (1971), 1208.
24. L. J. Kieffer, "A Compilation of Electron Collision Cross Section Data for Modeling Gas Discharge Lasers", JILA Information Center Report 13, September 1973.

25. M. K. Farnaam, "The Surface Chemistry of Epitaxial Silicon Deposition by Thermal Cracking of Silane, PhD Thesis, LBL-15448 (1983).

26. C. Gelain, A. Cassuto, P. LeGoff, Abstract of Bulletin of French Ceramic Society 80, 23 (1968).

27. J. V. Florio and W. D. Robertson, Surf. Sci. 22 (1970), 459.

28. J. J. Lander, Surf. Sci. 1 (1964), 125.

29. G. Lucovsky, J. Vac. Sci. Technol. 16 (1979), 1225.

FIGURE CAPTIONS

Fig. 1. Apparatus cross-section.

Fig. 2. Theoretical and experimental values of ε and ϕ vs. modulation frequency at 1243 K.

Fig. 3. Theoretical and experimental values of ε and ϕ vs. modulation frequency at 1443 K.

Fig. 4. Theoretical and experimental values of ε and ϕ vs. beam intensity.

Fig. 5. Theoretical and experimental values of ε and ϕ vs. reciprocal surface temperature.

Fig. 6. Silane phase lag with respect to argon vs. frequency in mixed beam high temperature experiments. Corrections for mass-dependent transit effects are shown.

Fig. 7. Best-fit and runner-up SiH_2 decomposition rate constants.

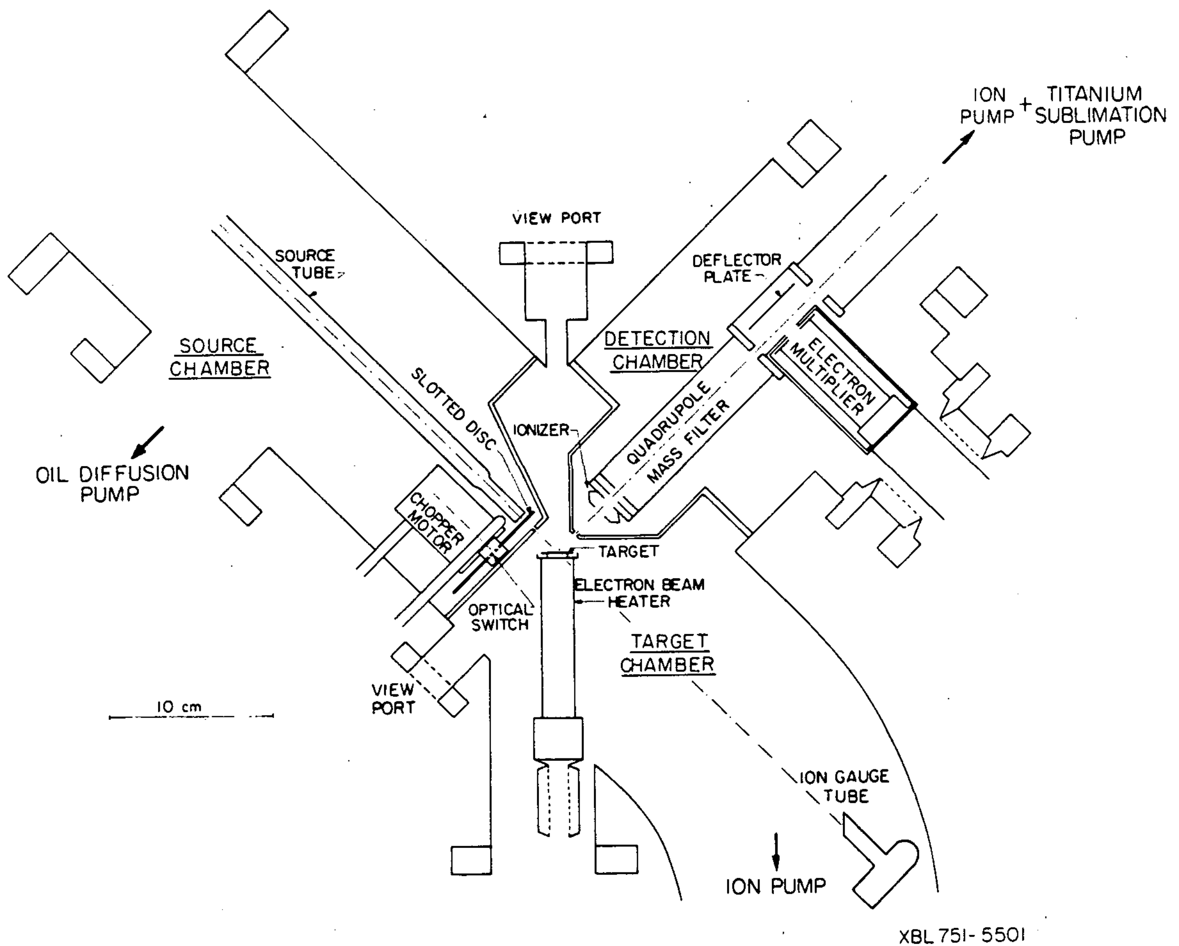

Fig. 1

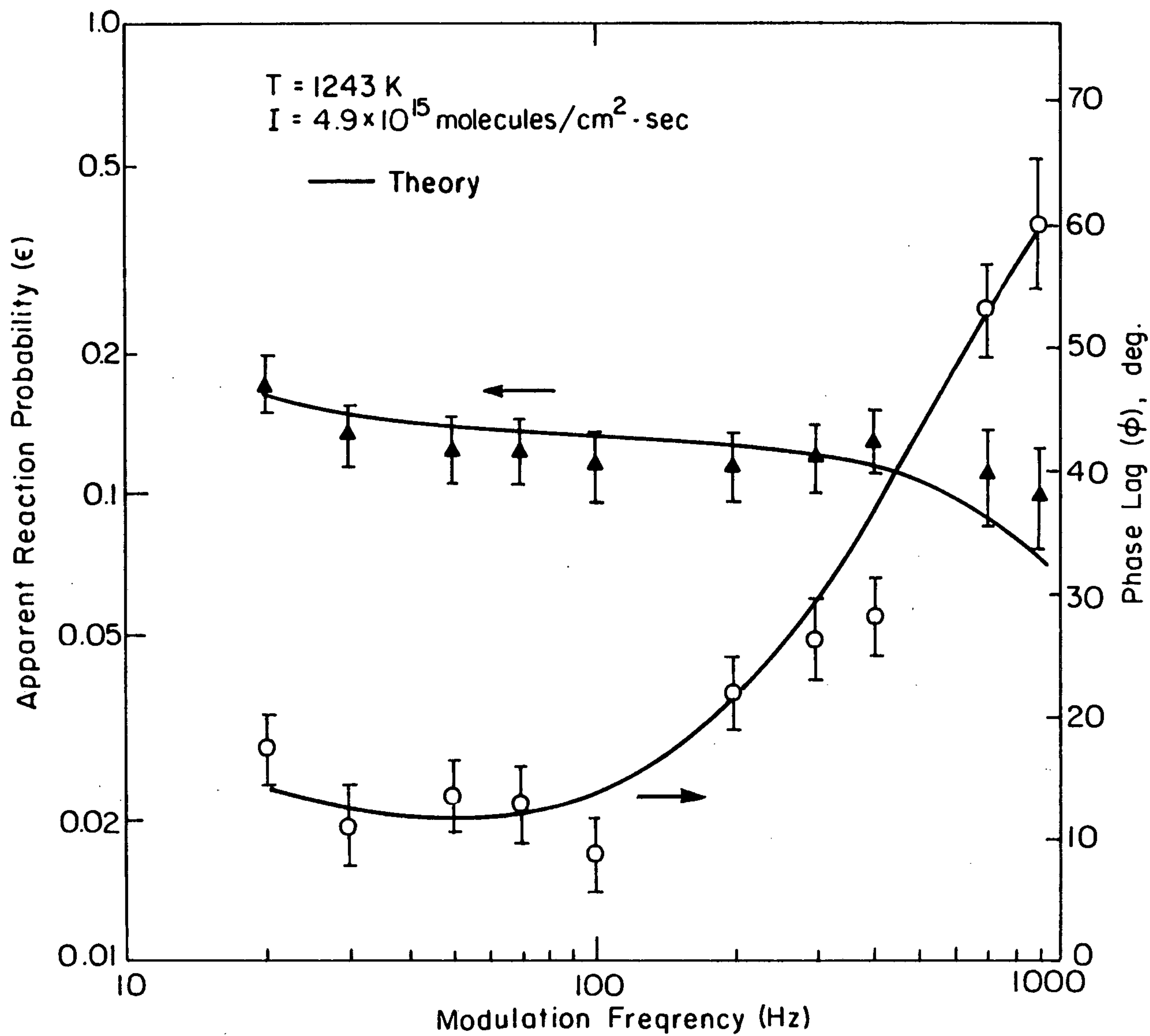

Fig. 2

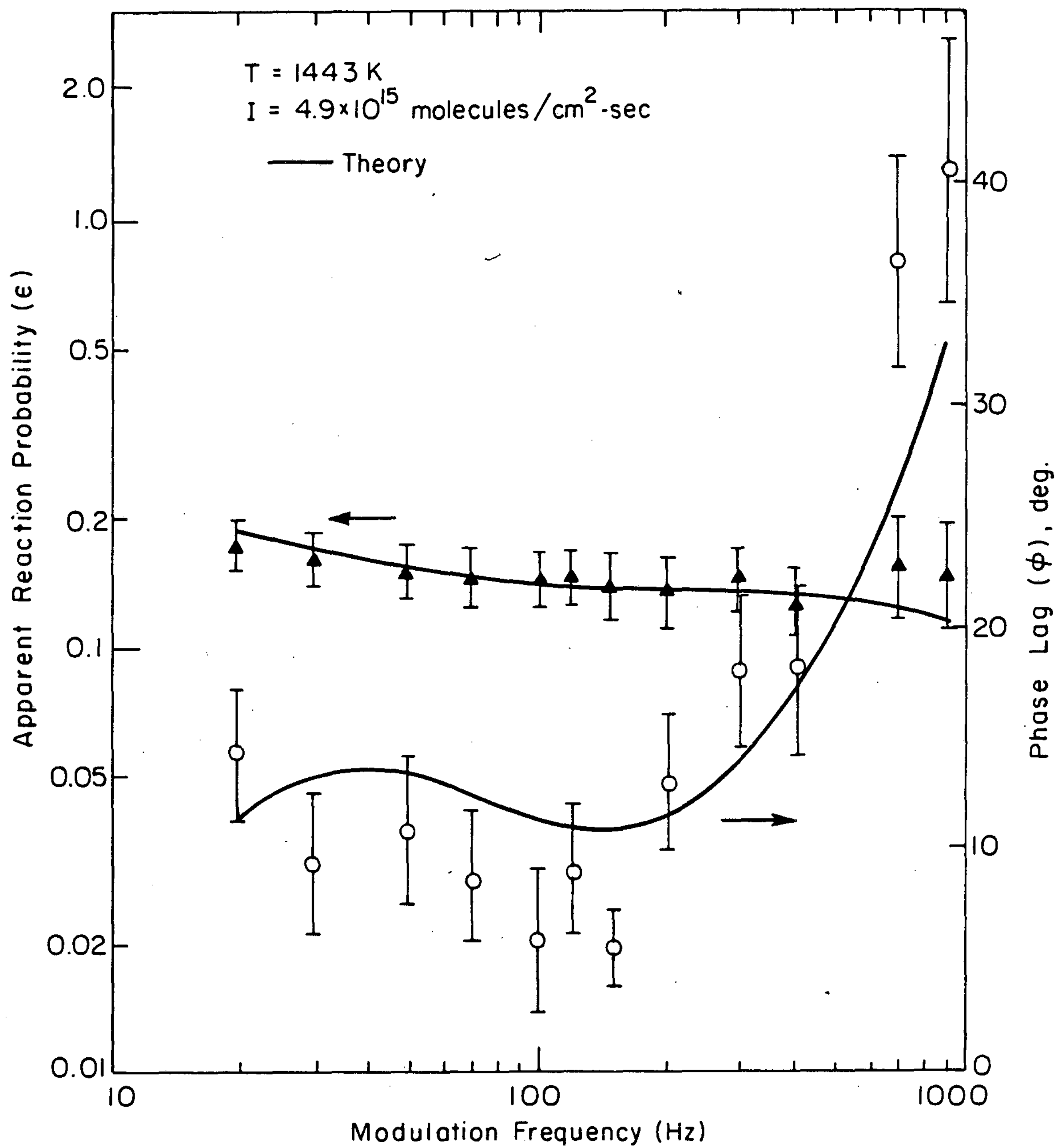

Fig. 3

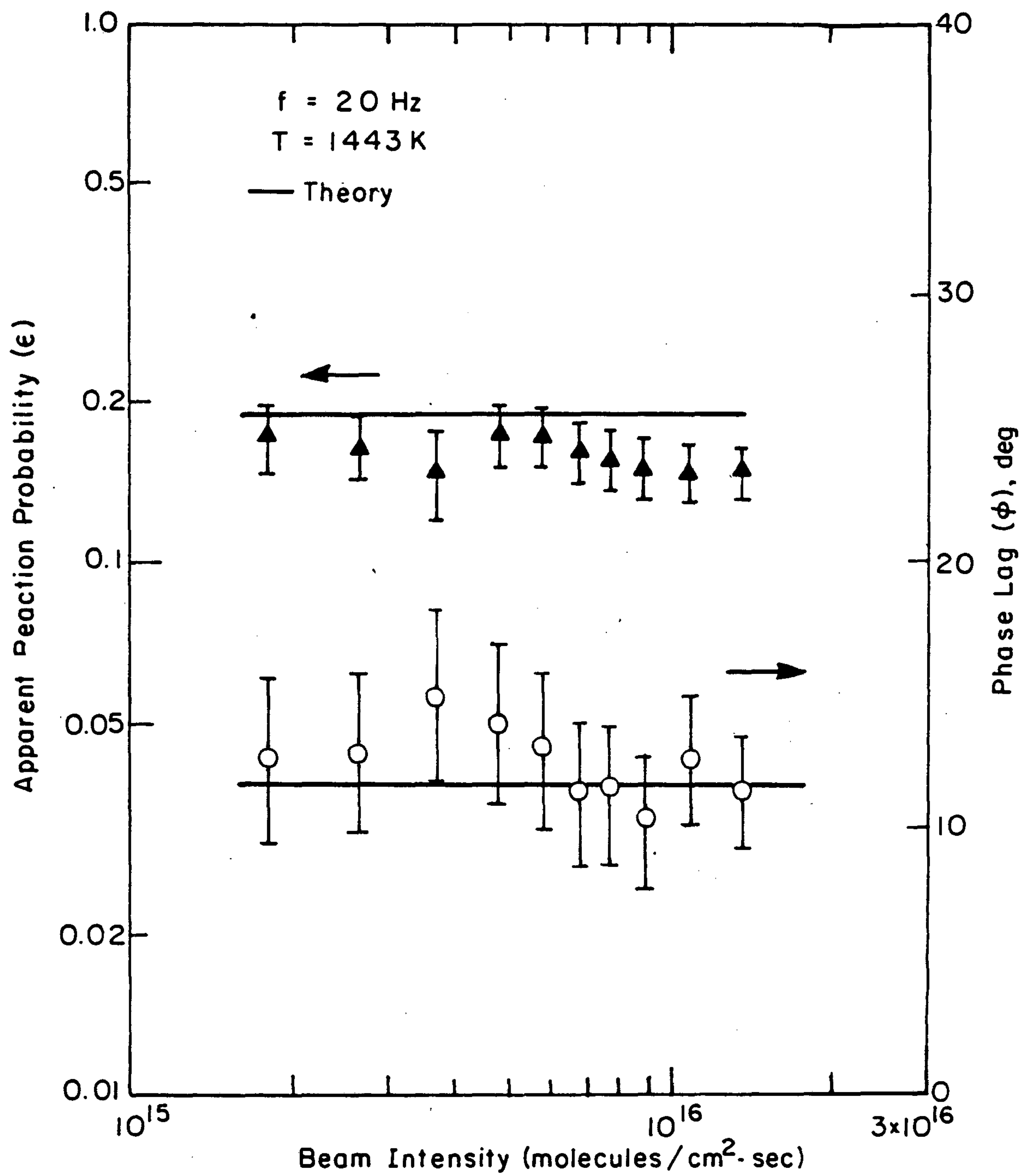

Fig. 4

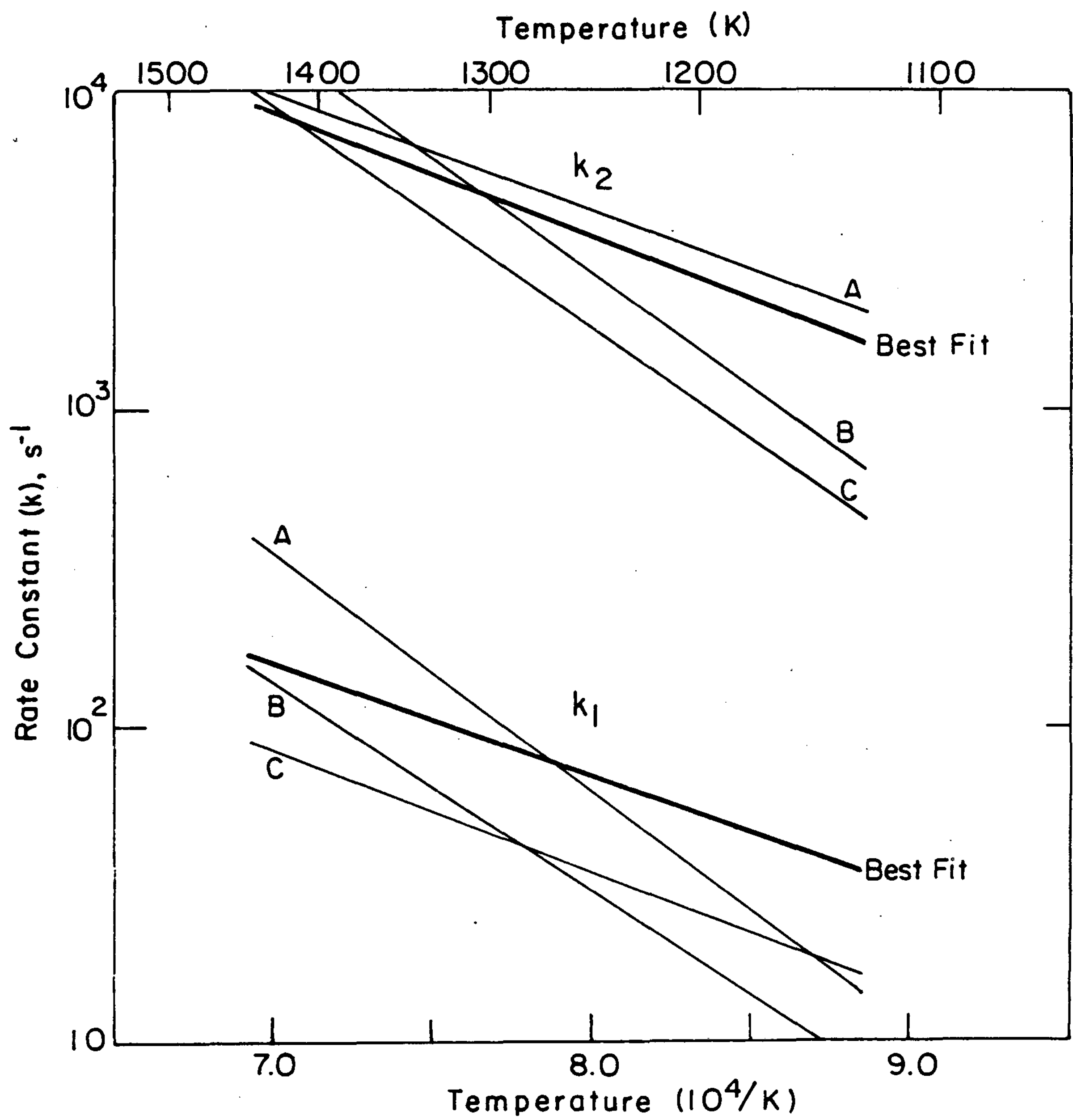

Fig. 5

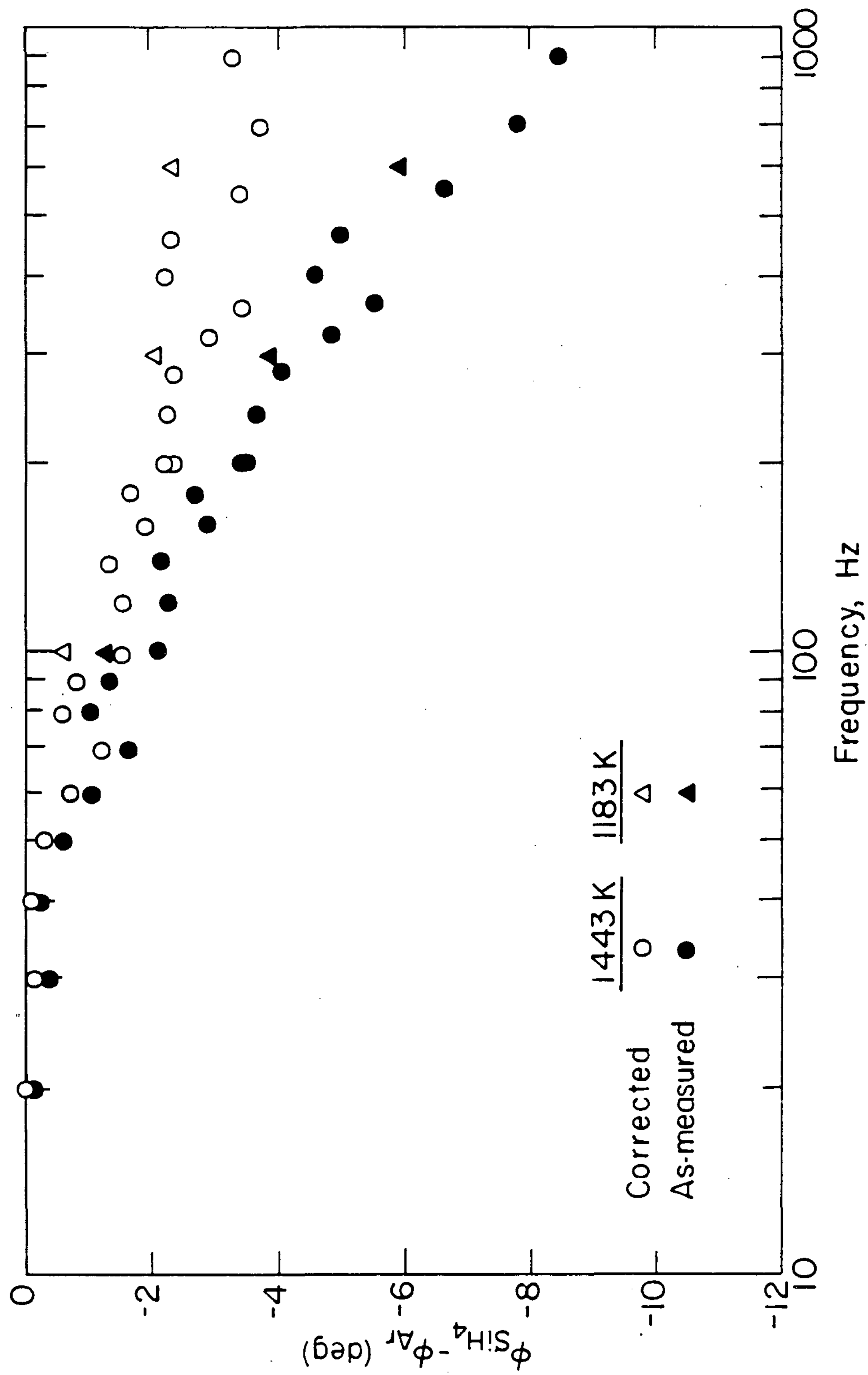

XBL 812-5282A

Fig. 6

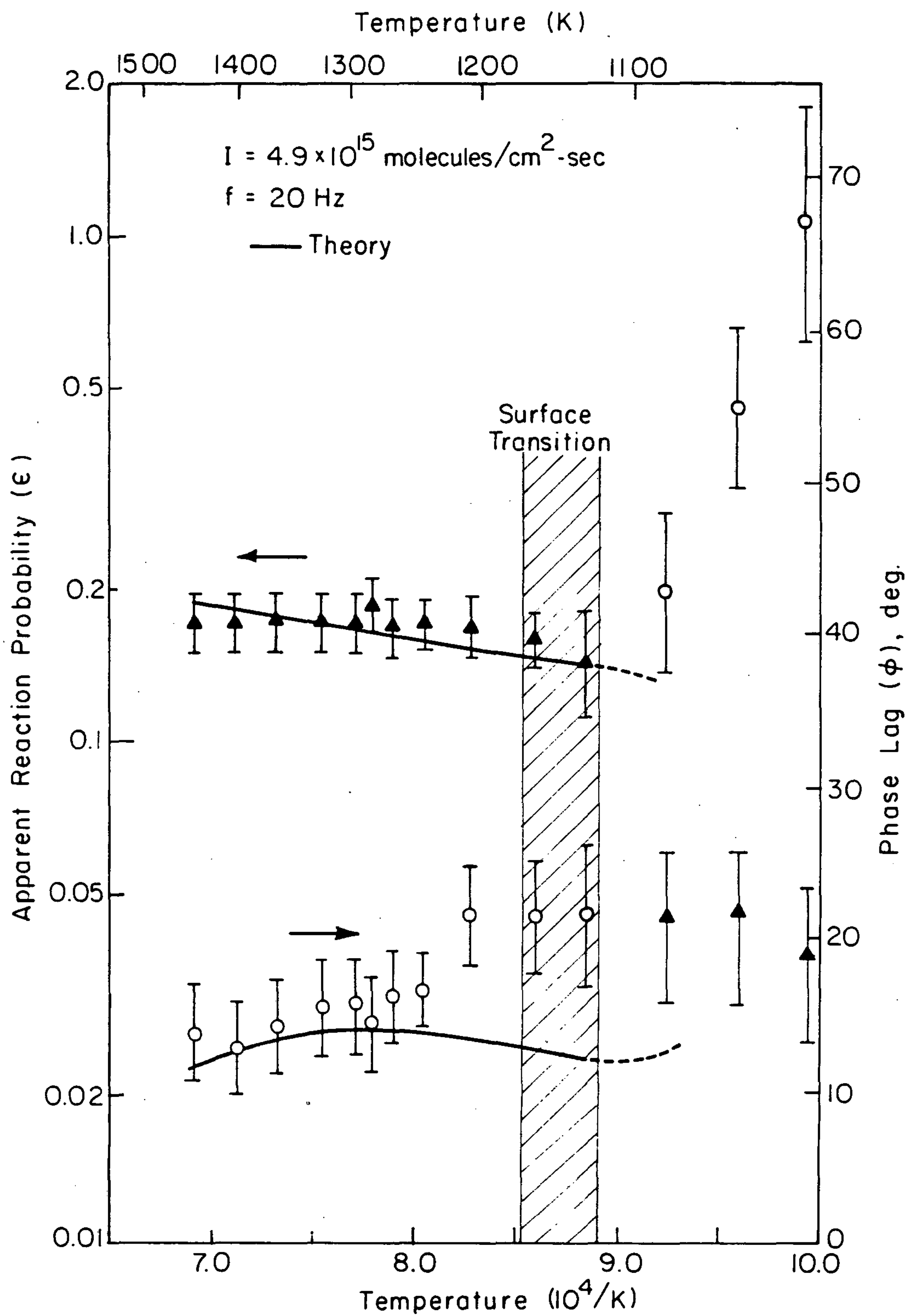

Fig. 7

This report was done with support from the Department of Energy. Any conclusions or opinions expressed in this report represent solely those of the author(s) and not necessarily those of The Regents of the University of California, the Lawrence Berkeley Laboratory or the Department of Energy.

Reference to a company or product name does not imply approval or recommendation of the product by the University of California or the U.S. Department of Energy to the exclusion of others that may be suitable.

TECHNICAL INFORMATION DEPARTMENT
LAWRENCE BERKELEY LABORATORY
UNIVERSITY OF CALIFORNIA
BERKELEY, CALIFORNIA 94720